

# The Radiological Feature of Anterior Occiput-to-Axis Screw Fixation as it Guides the Screw Trajectory on 3D Printed Models: A Feasibility Study on 3D Images and 3D Printed Models

*Ai-Min Wu, MD, Sheng Wang, MD, Wan-Qing Weng, MD, Zhen-Xuan Shao, MD, Xin-Dong Yang, MS, Jian-Shun Wang, MD, Hua-Zi Xu, MD, and Yong-Long Chi, MD*

**Abstract:** Anterior occiput-to-axis screw fixation is more suitable than a posterior approach for some patients with a history of posterior surgery. The complex osseous anatomy between the occiput and the axis causes a high risk of injury to neurological and vascular structures, and it is important to have an accurate screw trajectory to guide anterior occiput-to-axis screw fixation.

Thirty computed tomography (CT) scans of upper cervical spines were obtained for three-dimensional (3D) reconstruction. Cylinders (1.75 mm radius) were drawn to simulate the trajectory of an anterior occiput-to-axis screw. The imitation screw was adjusted to 4 different angles and measured, as were the values of the maximized anteroposterior width and the left-right width of the occiput (C0) to the C1 and C1 to C2 joints. Then, the 3D models were printed, and an angle guide device was used to introduce the screws into the 3D models referring to the angles calculated from the 3D images.

We found the screw angle ranged from  $\alpha_1$  (left:  $4.99 \pm 4.59^\circ$ ; right:  $4.28 \pm 5.45^\circ$ ) to  $\alpha_2$  (left:  $20.22 \pm 3.61^\circ$ ; right:  $19.63 \pm 4.94^\circ$ ); on the lateral view, the screw angle ranged from  $\beta_1$  (left:  $13.13 \pm 4.93^\circ$ ; right:  $11.82 \pm 5.64^\circ$ ) to  $\beta_2$  (left:  $34.86 \pm 6.00^\circ$ ; right:  $35.01 \pm 5.77^\circ$ ). No statistically significant difference was found between the data of the left and right sides. On the 3D printed models, all of the anterior occiput-to-axis screws were successfully introduced, and none of them penetrated outside of the cortex; the mean  $\alpha_4$  was  $12.00 \pm 4.11$  (left) and  $12.25 \pm 4.05$  (right), and the mean  $\beta_4$  was  $23.44 \pm 4.21$  (left) and  $22.75 \pm 4.41$  (right). No significant difference was found between  $\alpha_4$  and  $\beta_4$  on the 3D printed models and  $\alpha_3$  and  $\beta_3$  calculated from the 3D digital images of the left and right sides.

Editor: James Franklin Kellam.

Received: September 15, 2014; revised: October 6, 2014; accepted: October 7, 2014.

From the Department of Orthopaedics, Second Affiliated Hospital of Wenzhou Medical University, Zhejiang Spinal Research Center, Wenzhou, Zhejiang, People's Republic of China (A-MW, SW, W-QW, Z-XS, J-SW, H-ZX, Y-LC); and Department of Anatomy, Wenzhou Medical University, Wenzhou, Zhejiang, People's Republic of China (X-DY).

Correspondence: Yong-Long Chi and Sheng Wang, Department of Orthopaedics, Second Affiliated Hospital of Wenzhou Medical University, Zhejiang Spinal Research Center, 109# XueYuan Western Road, Wenzhou, Zhejiang 325000, People's Republic of China (e-mail: spinechi@163.com; wangthomas2002@163.com).

National Natural Science Foundation of China (81372014), Natural Science Foundation of Zhejiang Province (LY14H060008), and Science research project for undergraduate student of Wenzhou Medical University (WYX201401021).

The funders had no role in study design, data collection and analysis, decision to publish, or preparation of the manuscript.

All authors declare that they have no conflict of interest.

Copyright © 2014 Wolters Kluwer Health | Lippincott Williams & Wilkins. This is an open access article distributed under the Creative Commons Attribution License 4.0, which permits unrestricted use, distribution, and reproduction in any medium, provided the original work is properly cited. ISSN: 0025-7974

DOI: 10.1097/MD.0000000000000242

Aided with the angle guide device, we could achieve an optimal screw trajectory for anterior occiput-to-axis screw fixation on 3D printed C0 to C2 models.

(*Medicine* 93(28):e242)

**Abbreviations:** AP = viewanteroposterior view, C0 = occiput, C1 = the first cervical vertebra, C2 = the second cervical vertebra, CT = computed tomography, 3D = three-dimensional.

## INTRODUCTION

Various posterior occipitocervical fusion techniques have been reported,<sup>1,2</sup> which are based on posterior wires, rods, plates, and screws,<sup>3-6</sup> and these technique achieve good osseous fusion and have been widely used by spine surgeons.

In a number of clinical situations, such as in the case described by Dvorak et al<sup>7</sup> patients with a history of posterior surgery leading to disruption of osseous anatomy and significant posterior scar tissue, there are not sufficient landmarks to achieve safe and effective posterior stabilization; Dvorak et al<sup>7</sup> performed anterior occiput-to-axis screw fixation on the patient in their case study. Simultaneously, a biomechanical study showed that anterior occiput-to-axis screw fixation could achieve biomechanical stability comparable to that of posterior approaches.<sup>8</sup>

Compared to posterior surgery, which causes considerable damage to the extensor muscles as well as bleeding, anterior occiput-to-axis screw fixation could be performed by a percutaneous approach,<sup>9</sup> which has the advantages of being minimally invasive, causing less blood loss, and resulting in shorter hospital stays.

The following additional advantages of occiput-to-axis screw fixation are reported: the anterior approach could be performed more conveniently than the posterior approach; the supine position is better for reduction and stable recovery and prevents having to change the position after anesthesia; and the anterior approach might be more suitable for patients with pressure from anteroposterior compression.

The complex osseous anatomy between the occiput and the axis causes a high risk of injury to the neurological and vascular structure; to avoid these complications, it is important to have an accurate screw trajectory to guide the anterior occiput-to-axis screw fixation.

## METHODS AND MATERIALS

The research was performed following the Declaration of Helsinki principles and was approved by the Institutional Review Board of The Second Affiliated Hospital of Wenzhou

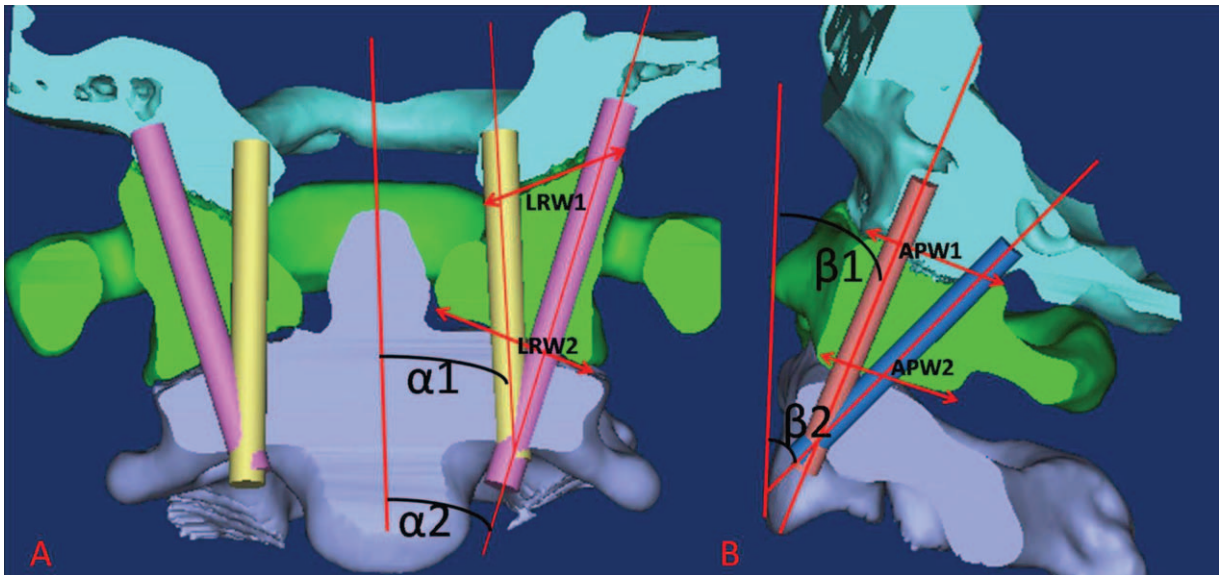


**FIGURE 1.** The schematic diagram (A and B) showing the methods of measurements for:  $\alpha 1$ : maximized interior angle on the AP view;  $\alpha 2$ : maximized lateral angle on the AP view;  $\beta 1$ : minimized dorsal angle on the lateral view;  $\beta 2$ : maximized dorsal angle on the lateral view; APW1 and LRW1: anteroposterior width and left-right width of the occiput (C0) to the C1 joint; APW2 and LRW2: anteroposterior width and left-right width of the occiput to the C1 to C2 joint.

Medical University. Informed consent was obtained from the participants.

Thirty computed tomography (CT) scans of upper cervical spines were obtained from the Star PACS system (INFINITT, Seoul, South Korea) of our hospital; the participants were without spinal diseases, and had CT scans for health testing or had presented with oral diseases; patients with any spinal abnormality such as a fracture or tumor were excluded.

The data from the CT scans (in DICOM format) were imported into Mimics software v10.01 (Materialise, Leuven, Belgium) for the three-dimensional (3D) reconstruction. We drew a cylinder (1.75 mm radius) to simulate the trajectory of the anterior occiput-to-axis screw.

The screw entry point was identified at the concavity on the anterior cortex of the C2 arch referred to by Lu et al<sup>10</sup> and the angle of the imitation screw was adjusted to 4 different angles with the following measurements: maximized interior angle ( $\alpha 1$ ) and maximized lateral angle ( $\alpha 2$ ) on the anteroposterior (AP) view, minimized dorsal angle ( $\beta 1$ ), and maximized

dorsal angle ( $\beta 2$ ) to the referential line on the lateral view (Figure 1). The values of the maximized anteroposterior width and the left-right width of the occiput (C0) to the C1 (APW1 and LRW1) and C1 to C2 joints (APW2 and LRW2) were measured as well (Figure 1).

The average of  $\alpha 1$  and  $\alpha 2$  was calculated and is referred to  $\alpha 3$ , and the average of  $\beta 1$  and  $\beta 2$  was calculated and named  $\beta 3$ . Simultaneously, the 3D images data were saved in .STL format and imported to Cura software. After a 3D digital model was created in Cura, we save it in G code format and imported it to a 3D Printer (3D ORTHO Waston Med, Inc., Changzhou, Jiangsu, China) to print the 3D model.

After the 3D model was printed, it was fixed in a holding device, and an angle guide device was used (Figure 2, Designed by YLC and SW); the K-wire angle was referred to  $\alpha 3$  and  $\beta 3$ , as previously calculated. After the K-wire was inserted with the assistance of the angle guide device, the AP and lateral X-ray films were obtained, the angle of the screw on the AP and lateral films were measured and referred to as  $\alpha 4$  and  $\beta 4$ , respectively.

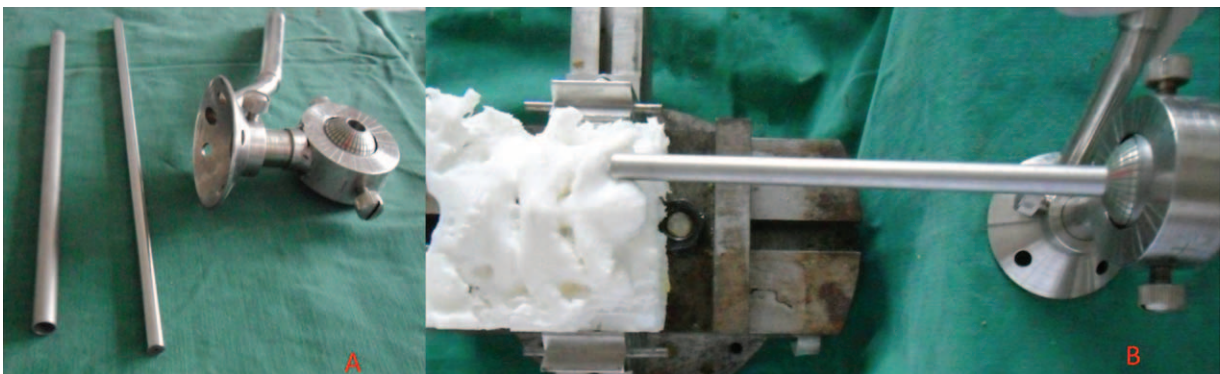


**FIGURE 2.** The photo of the angle guide device (A) and the method used to introduce the anterior occiput-to-axis screws on 3D printed models (B).

**TABLE 1.** The Parameters Measured From 3D Digital Images

		Left	Right	T	P-Value
AP view	α1 angle	4.99 ± 4.59	4.28 ± 5.45	0.858	0.398
	α2 angle	20.22 ± 3.61	19.63 ± 4.94	0.636	0.530
	α3 (averaged)	12.60 ± 3.73	11.95 ± 4.15	0.918	0.366
Lateral view	β1 angle	13.13 ± 4.93	11.82 ± 5.64	1.610	0.118
	β2 angle	34.86 ± 6.00	35.01 ± 5.77	-0.388	0.701
	β3(averaged)	23.86 ± 4.81	23.42 ± 4.89	0.530	0.600
C0–C1 facet	LRW1	12.43 ± 1.93	12.04 ± 2.17	1.721	0.096
	APW1	16.87 ± 1.34	16.88 ± 1.38	-0.075	0.940
C1–C2 facet	LRW2	15.92 ± 2.26	16.18 ± 2.00	-0.836	0.410
	APW2	15.76 ± 1.53	15.94 ± 1.56	-0.933	0.358

α1: Maximize interior angle on AP view; α2: maximize lateral angle on AP view; α3: the average of α1 and α2; β1: minimize dorsal angle on lateral view; β2: maximize dorsal angle on lateral view; β3: the average of β1 and β2; APW1 and LRW1: maximize anteroposterior width left-right width of occiput to C1 joint; APW2 and LRW2: maximize anteroposterior width and left-right width of occiput to C1 to C2 joint.

Then, the α4 and β4 measured in the 3D models were compared to α3 and β3.

**STATISTICAL ANALYSIS**

The statistical analysis was conducted using SPSS software v17.0 (SPSS, Inc., Chicago, IL). A paired *t*-test was used to compare the measurements of the left and right side and the measurements between the 3D digital images and the 3D printed models. The level of significance was set at *P* < 0.05.

**RESULTS**

On the AP view, the screw angle ranged from α1 (left: 4.99 ± 4.59°; right: 4.28 ± 5.45°) to α2 (left: 20.22 ± 3.61°; right: 19.63 ± 4.94°); on the lateral view, the screw angle ranged from β1 (left: 13.13 ± 4.93°; right: 11.82 ± 5.64°) to β2 (left: 34.86 ± 6.00°; right: 35.01 ± 5.77°). The anteroposterior width of the C0 to C1 facet was 16.87 ± 1.34 (left) and 16.88 ± 1.38 (right), slightly larger than that at the C1 to C2 facet (left: 15.76 ± 1.53) and 15.94 ± 1.56 (right); the left-right width of the C0 to C1 facet was 12.43 ± 1.93 (left) and 12.04 ± 2.17 (right), shorter than that at the C1 to C2 facet (left: 15.92 ± 2.26) and 16.18 ± 2.00 (right); they were all wide enough for 3.5 mm or 4.0 mm diameter anterior occiput-to-axis screw fixation. No statistically significant difference was found between the data of the left side and right side (Table 1).

Guided by the angles of α3 and β3 calculated from the 3D digital images and assisted with the angle guide device, all of the anterior occiput-to-axis screws were successful introduced and none of them penetrated outside of the cortex (Figure 3); the mean α4 was 12.00 ± 4.11 (left) and 12.25 ± 4.05 (right) and the mean β4 was 23.44 ± 4.21 (left) and 22.75 ± 4.41 (right). No significant difference was found between the α4 and β4 from the 3D printed models and the α3 and β3 calculated from the 3D digital images on the left and right sides (Table 2).

**DISCUSSION**

Occipitocervical fixation has been challenging for spinal surgeons because of the complex anatomical structures and the high risk of neural and vascular injury at the occipitocervical junction.<sup>11,12</sup> Most previous reports focused on posterior

techniques based on rods, plates, and screws to achieve occipitocervical fusion.<sup>3,4,6</sup>

Posterior stabilization is not suitable in a number of unique situations, such as that of patients with a history of posterior surgery leading to disruption of the osseous anatomy and significant posterior scar tissue, described by Dvorak et al<sup>7</sup> and that of patients with a history of posterior cranial fossa decompression surgery or dysplastic C2 pedicles, described by Wu et al<sup>9</sup> Anterior occiput-to-axis screw fixation could be performed via the Smith–Robinson approach or percutaneously; compared to the posterior approach, which causes considerable damage to the extensor muscles and bleeding, the anterior approach is less invasive and results in less blood loss. Cai et al<sup>13</sup> reported a novel anterior occiput-to-axis locking plate system, which might have a better biomechanical property than simply 2 anterior occiput-to-axis screws; however, their

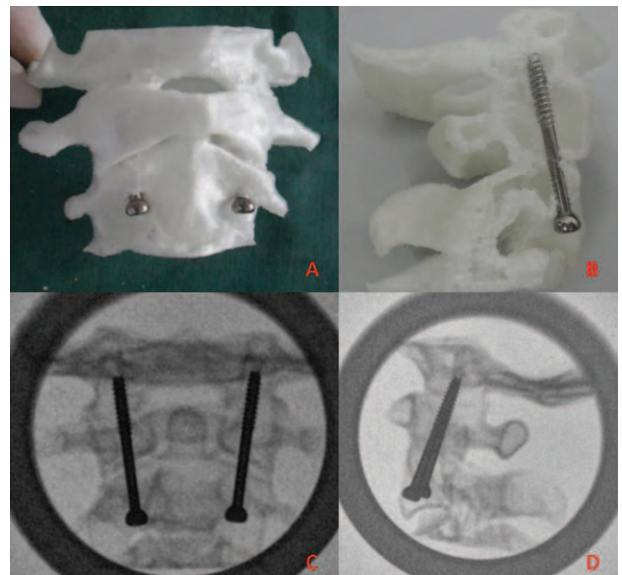


**FIGURE 3.** The photo of the 3D printed models after the anterior occiput-to-axis screws were introduced (A and B), the AP (C) and lateral (D) X-ray films of the 3D printed models after the anterior occiput-to-axis screws were introduced.

**TABLE 2.** The Comparison of Angles Between 3D Digital Images and 3D Printed Models

		$\alpha 3$ or $\beta 3$	$\alpha 4$ or $\beta 4$	<i>T</i>	<i>P</i> -Value
AP view	Left	12.60 ± 3.73	12.00 ± 4.11	-1.565	0.128
	Right	11.95 ± 4.15	12.25 ± 4.05	1.013	0.320
Lateral view	Left	23.86 ± 4.81	23.44 ± 4.21	-0.960	0.345
	Right	23.42 ± 4.89	22.75 ± 4.41	-1.724	0.095

$\alpha 3$ : The average of  $\alpha 1$  and  $\alpha 2$ ;  $\beta 3$ : the average of  $\beta 1$  and  $\beta 2$ ;  $\alpha 4$ : the angle of screw in 3D printed models on AP view;  $\beta 4$ : the angle of screw in 3D printed models on lateral view.

technique is based on 2 anterior occiput-to-axis screws. It is important to analyze the anatomic parameters of anterior occiput-to-axis screw fixation and to establish an accurate method of guiding the optimal screw trajectory.

With the data from the CT scans, we could reconstruct 3D digital images and use a cylinder to imitate the screw trajectory.<sup>14</sup> Puchwein et al<sup>15</sup> performed morphometry of the odontoid peg on 3D digital images, and their data were valuable for guiding anterior odontoid screw fixation and informing surgeons on the selection of 1 or 2 anterior odontoid screws.

Our previous study showed that 3D printed models accurately shaped the 3D digital images (data not shown in this study) and is suitable for spinal fixation research. In our study, we used the  $\alpha 3$  and  $\beta 3$  calculated from the 3D digital images as the reference and the angle guide device to introduce the anterior occiput-to-axis screws. We found that our method could guide an optimal screw trajectory, and none of the screws in this study penetrated outside of bone cortex.

CT-based navigation was developed in recent decades,<sup>16,17</sup> and its use could enable accurate screw placement; however, the navigation system is excessively expensive for most hospitals. A worldwide survey found that<sup>18</sup>: despite widespread distribution of the navigation system in North America and Europe, 11% of surgeons use these systems routinely; the lack of equipment, inadequate training, and high costs were the major reasons that the nonusers do not use the navigation systems. The rate of having and using navigation systems in developing countries was less than that in developed countries. Our novel angle guide device is much less expensive than the navigation system, with simple construction and methodology that is relatively easy to learn. The device has potential value for surgeons who do not have access to the expensive navigation system. Further study of this novel angle guide device in clinical practice is needed.

## CONCLUSION

There was enough space for anterior occiput-to-axis screw fixation, and by referring to the parameters of optimal screw trajectory and with the aid of the angle guide device, we could achieve an optimal screw trajectory on a 3D printed C0 to C2 model.

## REFERENCES

1. Winegar CD, Lawrence JP, Friel BC, et al. A systematic review of occipital cervical fusion: techniques and outcomes. *J Neurosurg Spine*. 2010;13:5–16.
2. Finn MA, Bishop FS, Dailey AT. Surgical treatment of occipitocervical instability. *Neurosurgery*. 2008;63:961–968, discussion 968–969.
3. Abumi K, Takada T, Shono Y, et al. Posterior occipitocervical reconstruction using cervical pedicle screws and plate-rod systems. *Spine (Phila Pa 1976)*. 1999;24:1425–1434.
4. Deen HG, Birch BD, Wharen RE, Reimer R. Lateral mass screw-rod fixation of the cervical spine: a prospective clinical series with 1-year follow-up. *Spine J*. 2003;3:489–495.
5. Grob D. Posterior occipitocervical fusion in rheumatoid arthritis and other instabilities. *J Orthop Sci*. 2000;5:82–87.
6. Vender JR, Rekito AJ, Harrison SJ, McDonnell DE. The evolution of posterior cervical and occipitocervical fusion and instrumentation. *Neurosurg Focus*. 2004;16:E9.
7. Dvorak MF, Fisher C, Boyd M, et al. Anterior occiput-to-axis screw fixation: part I: a case report, description of a new technique, and anatomical feasibility analysis. *Spine (Phila Pa 1976)*. 2003;28:E54–E60.
8. Dvorak MF, Sekeramayi F, Zhu Q, et al. Anterior occiput to axis screw fixation: part II: a biomechanical comparison with posterior fixation techniques. *Spine (Phila Pa 1976)*. 2003;28:239–245.
9. Wu AM, Chi YL, Weng W, et al. Percutaneous anterior occiput-to-axis screw fixation: technique aspects and case series. *Spine J*. 2013;13:1538–1543.
10. Lu J, Ebraheim NA, Yang H, et al. Anatomic considerations of anterior transarticular screw fixation for atlantoaxial instability. *Spine (Phila Pa 1976)*. 1998;23:1229–1235, discussion 1236.
11. Neo M, Fujibayashi S, Miyata M, et al. Vertebral artery injury during cervical spine surgery: a survey of more than 5600 operations. *Spine (Phila Pa 1976)*. 2008;33:779–785.
12. Elliott RE, Tanweer O, Boah A, et al. Comparison of screw malposition and vertebral artery injury of c2 pedicle and transarticular screws: meta-analysis and review of the literature. *J Spinal Disord Tech*. 2014;27:305–315.
13. Cai X, Yu Y, Liu Z, et al. Three-dimensional finite element analysis of occipitocervical fixation using an anterior occiput-to-axis locking plate system: a pilot study. *Spine J*. 2014;14:1399–1409.
14. Wu AM, Tian NF, Wu LJ, et al. A radiological and cadaveric study of oblique lumbar interbody fixation in patients with normal spinal anatomy. *Bone Joint J*. 2013;95-B:977–982.
15. Puchwein P, Jester B, Freytag B, et al. The three-dimensional morphometry of the odontoid peg and its impact on ventral screw osteosynthesis. *Bone Joint J*. 2013;95-B:536–542.
16. Singh PK, Garg K, Sawarkar D, et al. Computed tomography-guided c2 pedicle screw placement for treatment of unstable hangman fractures. *Spine (Phila Pa 1976)*. 2014;39:E1058–E1065.
17. Tian NF, Xu HZ. Image-guided pedicle screw insertion accuracy: a meta-analysis. *Int Orthop*. 2009;33:895–903.
18. Hartl R, Lam KS, Wang J, et al. Worldwide survey on the use of navigation in spine surgery. *World Neurosurg*. 2013;79:162–172.